Calibration of the absorptance cavities for the spaceflight solar radiometer TIM

Karl Heuerman, David Harber, Allison Ebbets, Greg Kopp, and Lucy Logan
Laboratory for Atmospheric and Space Physics, University of Colorado
1234 Innovation Drive, Boulder, CO 80303

ABSTRACT

The Total Irradiance Monitor (TIM) is a total solar irradiance radiometer on NASA's SORCE mission launched in 2003 and on the NASA/Glory mission launching in 2008. The primary sensors in TIM must absorb energy with accurately calibrated efficiency across the entire solar spectrum. To achieve high efficiency and good thermal conduction, the four sensors in each instrument are hollow conical silver cavities with a cylindrical entrance extension and a diffuse black nickel phosphorous (NiP) interior that converts absorbed incident radiation to thermal energy. A stable resistive heater wire embedded in the cone along with thermistors mounted on the cavity exterior are used in a temperature-sensing servo loop to measure the spectrally-integrated incident solar radiation. Characterization of the absorptance properties of the cavities across the solar spectrum is a dominant driver of instrument accuracy, and a dedicated facility has been developed to acquire these calibrations with uncertainties of approximately 50 ppm (0.005%). This paper describes the absorptance calibration facility, presents the preliminary cavity reflectance results for the Glory mission's TIM instrument, and details the uncertainty budget for measuring these cavity reflectances.

Keywords: Glory, TIM, absorptance, reflectance, solar irradiance, ESR

1. Introduction

TIM is an ambient temperature, electrical substitution solar radiometer designed to achieve 100 parts per million (ppm) relative standard uncertainty in total solar irradiance (TSI). The TIM contains four cone shaped electrical substitution radiometers (ESRs), which are electrically heated to maintain constant temperature while a shutter modulates sunlight through a precision aperture and into the absorptive cavity. The modulation in electrical heater power needed to maintain an ESR's temperature as its shutter modulates incident sunlight indicates the radiative power absorbed by that cavity [1].

At this time there is no facility able to calibrate the TIM end-to-end at the level of accuracy for which the instrument is designed. In lieu of end-to-end calibrations at the instrument level, precision calibrations of components and subsystems yield the uncertainty budget for the instrument [2]. One such component of the TIM uncertainty budget is the cavity absorptance (α). This calibration parameter has its own uncertainty budget, which is presented in this paper. This budget outlines the sources of uncertainty in the cavity absorptance measurement, and the root sum square (RSS) of the individual sources then yields the total uncertainty of the measurement. The quantity actually measured with the facility is cavity reflectance which is $1 - \alpha$; discussion in this paper may use either term since one quantity defines the other. While this paper specifically discusses the reflectance measurements of the TIM cavities, the approach is applicable to other highly-absorptive objects.

The inverse of the cavity absorptance enters in the measurement equation that converts the digital numbers output from TIM to the solar irradiance [1]. With a goal of 100 ppm (0.01%) uncertainty for the entire instrument, individual calibrations need to be kept small. For the SORCE instrument the ground based calibrations of the cone absorptance along with the aperture area made the largest contributions to the instrument budget and have thus received increased attention for Glory. Once in flight the absorptance can be monitored for relative changes by comparisons with other cavities and by an independent photodiode looking into cavity to track the stability over the life of the mission. Corrections for changing reflectivity can be made in ground processing to mitigate the degradation caused by solar exposure; however, the only absolute calibrations of cavity absorptance come from ground calibrations.

Earth Observing Systems XI, edited by James J. Butler, Jack Xiong,
Proc. of SPIE Vol. 6296, 62961H, (2006) · 0277-786X/06/$15 · doi: 10.1117/12.679668

2. Radiometer cavity design

The TIM ESR cavities (see Fig. 1) are the primary sensors in the instrument and are designed to efficiently absorb incoming solar radiation. The cone shape directs any specular reflectance from incident light deeper into the cavity for additional impacts on the absorptive cavity wall. The cone interior is a diffuse surface of etched black Nickel Phosphorous (NiP), which creates a labyrinth of voids that trap light of nearly all wavelengths. Since the NiP is a metal it provides excellent thermal conductivity to the cone substrate, speeding the thermal time response of the cavity, and has a high damage threshold to UV radiation as compared to organic based black paints.

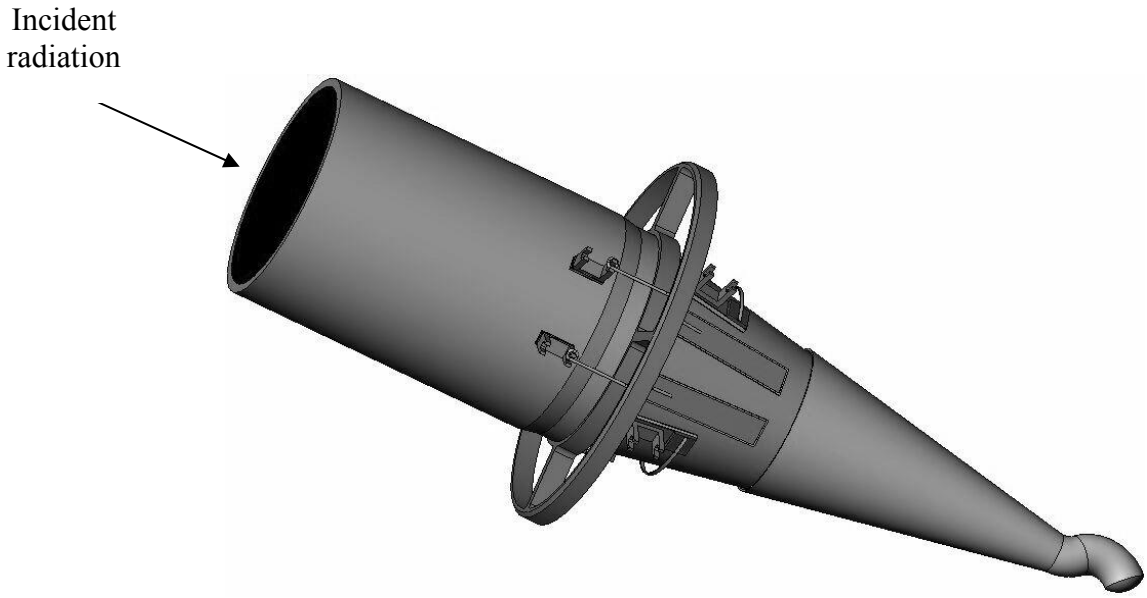

Fig. 1. The TIM radiometer cavities are designed to efficiently trap incident sunlight.

3. Reflectance measurement facility

Cavity reflectance ($1-\alpha$) is measured using laser scans mapping the cavity interiors at seven wavelengths spanning the spectral peak of the incident solar flux. These spatially resolved measurements are supplemented by spatially integrated calibrations at 10.6 μm to extend the spectral coverage. The effective cavity reflectance for solar irradiance measurements is the average of the reflectance measurements at individual wavelengths weighted by the solar energy distribution given by Lean [3]. A spatial map of cavity reflectance from a 2-dimensional laser scan is averaged over the region of the cone illuminated by sunlight to obtain the effective reflectance at that laser wavelength. The effects of the spatially-extended (0.5 degree angular extent) Sun and solar limb-darkening are accounted for when computing these spatial reflectance averages. A spatial map, such as that shown in Fig. 2, is acquired at each of seven laser wavelengths (457, 532, 633, 850, 1064, 1523, and 3390 nm) spanning the primary solar spectrum.

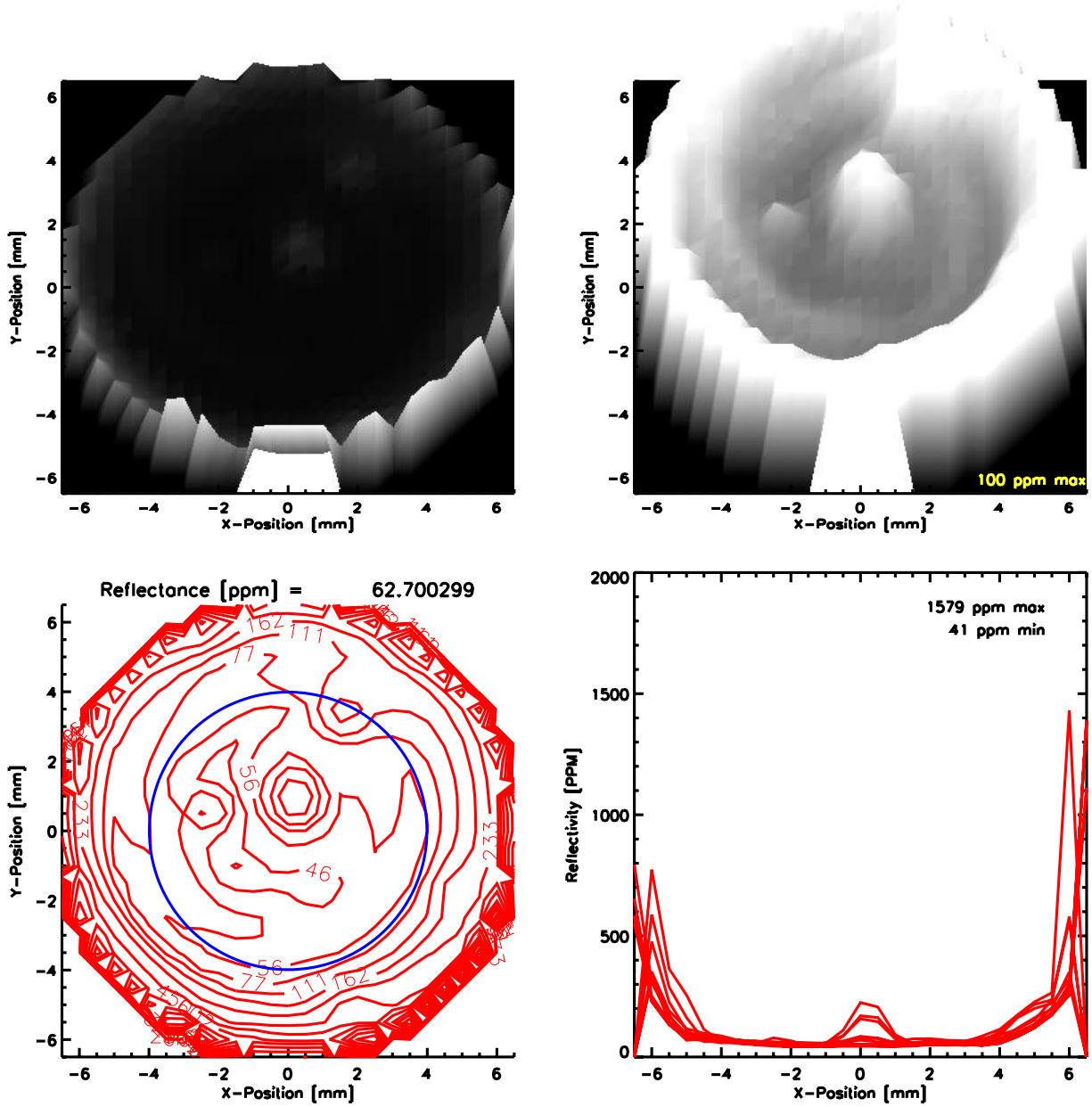

Fig. 2. The spatial map of the cavity reflectance at 633 nm indicates the spatial variations in cavity reflectance. An average over the illuminated portion of the cavity gives the effective reflectance at this wavelength (lower left plot).

The spatially resolved laser measurements are supplemented by a spatially integrated measurement at 10.6 microns to extend the reflectance calibrations to the mid-infrared. Additionally, NIST FTIR measurements from 2 to 20 microns of select SORCE/TIM cavities, described by Hanssen [4], fill in the spectral gaps between the discrete laser wavelengths, and show that the cavity reflectance varies smoothly with wavelength through the mid-infrared.

The cavity reflectances are smoothly fitted between the discrete laser calibration wavelengths. The integral over wavelength of this fit to the reflectances weighted by the solar spectrum gives the solar-weighted average reflectance for each cavity (see Fig. 6).

A schematic of the reflectance measurement facility is shown in Fig. 3. A laser source is first sent through a beam splitter that directs a small fraction of the beam to a monitor photodiode. The monitor signal is used to correct for significant intensity variations that were exhibited by some of the lasers. The beam then passes through a chopper that modulates the laser at 90 Hertz and provides a suitable signal for the Stanford Research Systems lock-in amplifier. Finally, the laser passes through a small aperture in the custom-made photodiode array and illuminates the cone cavity that is mounted on a 2-axis platform. Radiation reflected out of the cone cavity is measured by the cavity-facing diode array. The signal from the photodiode array is sent to the lock-in amplifier, and phase sensitive detection is used to separate the reflected laser light from other background sources. Different detector arrays are used at different wavelengths to respond to the lasers spanning the solar spectrum: Silicon is used for 457 nm through 1064 nm, Germanium for 1523 nm, and Lead Selenide for 3390 nm.

The advantage of this technique, as opposed to the use of an integrating sphere or a hemisphere as is used for the integrated reflectance 10.6 μm measurement, is that the reflected radiation is detected with high efficiency by the photodiode array, and thus small amounts of reflected light can be measured with high a signal-to-noise ratio. Additionally, by mounting the cone on an X-Y stage, a spatial map of the cone reflectance can be obtained.

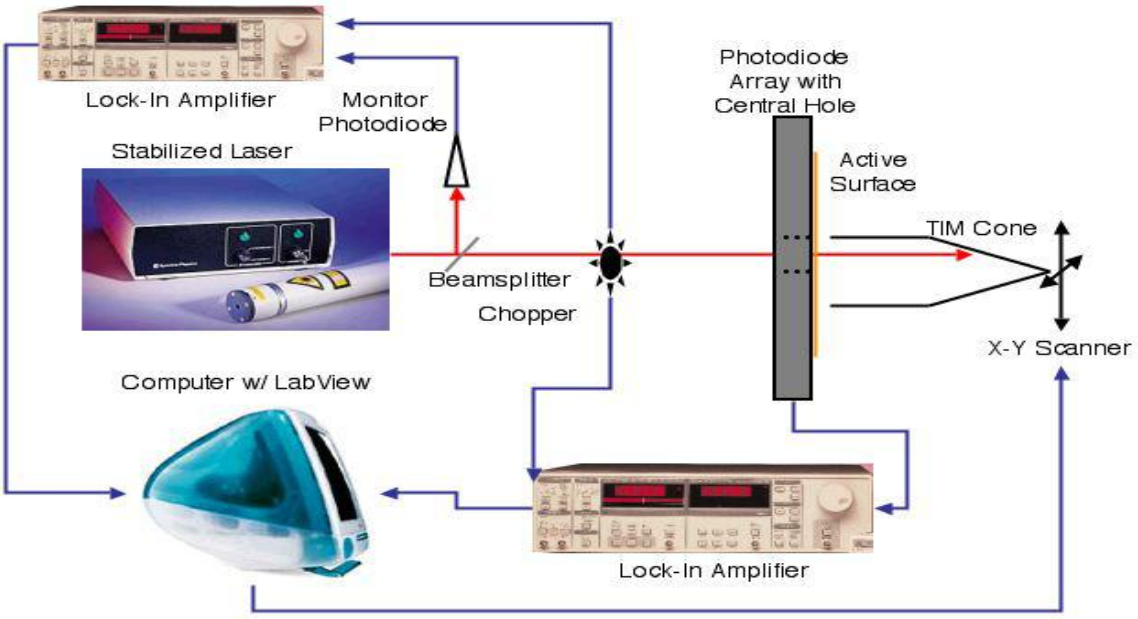

Fig. 3. Schematic of the cone reflection facility shows the beam path traveling from the laser to the cone mounted on a 2-axis stage. The lock-in amplifier uses phase sensitive detection to reduce sensitivity to background sources.

4. Spatially mapped reflectance

The spatial reflectance of a cavity is computed from a raster scan of the cavity normalized by the detector sensitivity over the region illuminated by the light reflected from the cavity, which varies with cavity position. This normalization requires knowledge of the spatial response uniformity of the detector array, which is determined by scanning the laser

over the detector array oriented to directly view the incident beam; this sensitivity map determines both the sensitivity of the detector elements and the geometry of the array.

To scan the interior of a cavity, a stationary and chopped laser beam is incident on the cavity interior as the cavity is scanned in two dimensions. The light scattered out of the cavity is measured by a stationary detector array in close proximity to the cavity mouth. The detector arrays used have a small central hole allowing the laser beam to pass through and illuminate the cavity while the array captures the majority of the light exiting the cavity. A raster at 0.5 mm point spacing covers the entire interior of the cone. The exiting light is analyzed at the chopper frequency of roughly 90 Hz to reduce sensitivity to background sources. The stability of the laser beam is monitored so that corrections for intensity can be made if needed.

To acquire absolute reflectance measurements, the detector array signal from a scan of a cavity must be normalized by the detector sensitivity over the region of the array that collected the light reflected from the cavity interior. To determine the sensitivity map of the detector, the detector array is attached to the X-Y stage and rotated to face the laser. With a low gain setting on the preamplifier, the entire active area is raster scanned with 0.5 mm spacing between points while recording the signal from the incident laser beam at each point. At each raster point the detector sensitivity is averaged over all the raster points that fall within 7.6 mm of that point, encompassing the area illuminated if a cone were placed in front of the detector; this is essentially a convolution of the detector sensitivity with the entrance area to the cavity. An effective detector sensitivity map (Fig. 4) is then generated, which gives the average sensitivity of the detector for a cone placed at each raster position.

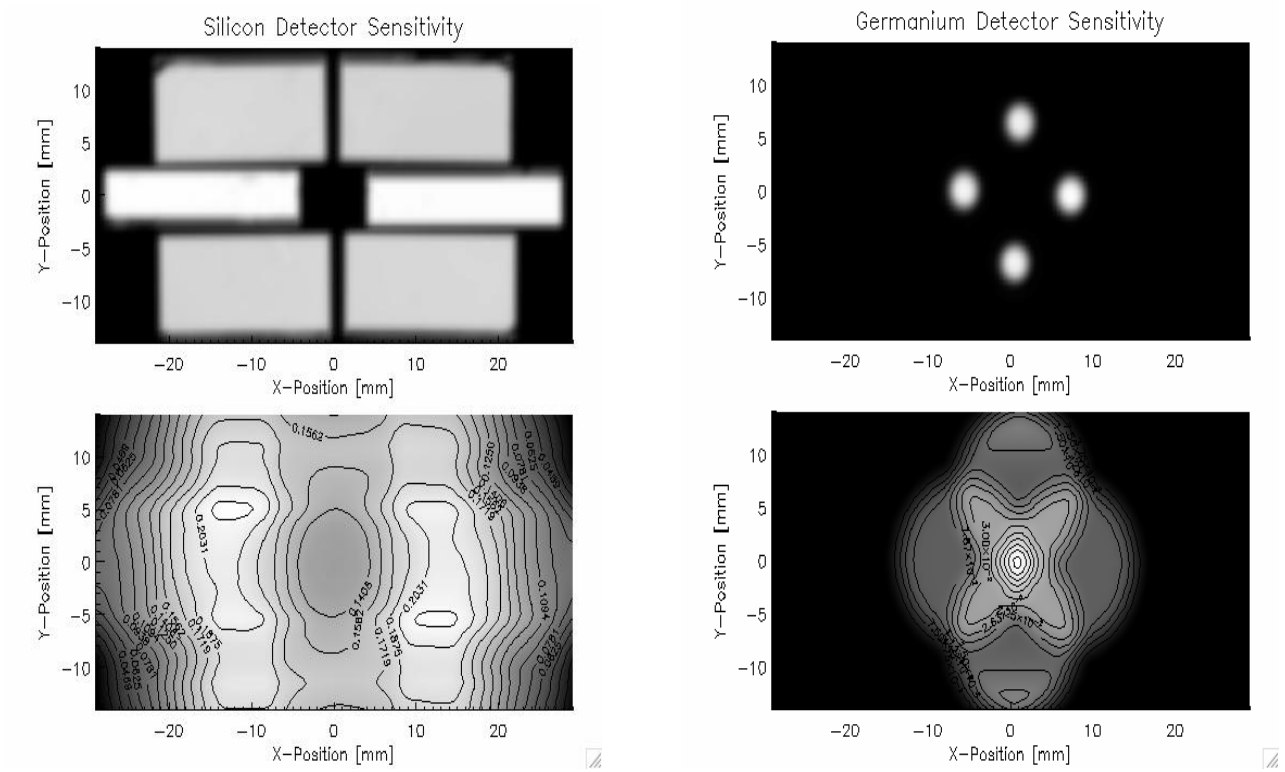

Fig. 4. Raster scans for a silicon and germanium detector (top panels) and the respective detector sensitivity maps created (bottom) by spatially averaging the detector response over the region illuminated by light reflected from a cone.

A ratio of the cone raster scan to the sensitivity map multiplied by the ratio of the electronic gains for each scan yields the effective reflectance of the cone cavity. A general representation for light scattering from a cone is given by the equation:

$$R_{0,cone} = \frac{1}{A} \cdot \frac{Gain_{Det}}{Gain_{cone}} \cdot \frac{Signal_{cone}}{Signal_{Det}} \cdot \frac{\int_{Aperture} QE(A) \cdot dA}{\int_{Aperture} Scatter_{cone}(A) \cdot QE(A) \cdot dA}$$

where:

R = Reflected component (1 – Absorptance)
A = Collecting aperture area (cavity mouth)
Gain = gain of the processing electronics for the cone and the detector scans
QE = relative measure of the detector efficiency

If the reflected light out of the cone is assumed to be spatially uniform, as it should be based on analyses of BRDF measurements of the diffuse NiP on the cavity interiors, this can be reduced to:

$$R_{0,cone} = \frac{Gain_{Det}}{Gain_{cone}} \cdot \frac{Signal_{cone}}{Signal_{Det}}$$

Thus, the cone reflectance can be determined by multiplying the gain ratio to the cone raster scan divided by the sensitivity map.

5. Spatially integrated reflectance

For the 10.6 μm laser a spatially integrated reflectance, rather than a spatially mapped reflectance, was measured. Due to the low signal-to-noise ratio for detection of 10.6 μm radiation, this wavelength was not well suited to the spatially mapped reflectance measurement previously described. Instead, a hemispherical reflector was used in order to concentrate the radiation reflected from the cone onto a single detector. This method, however, provides only a single number and not a spatial map of the cone reflectance.

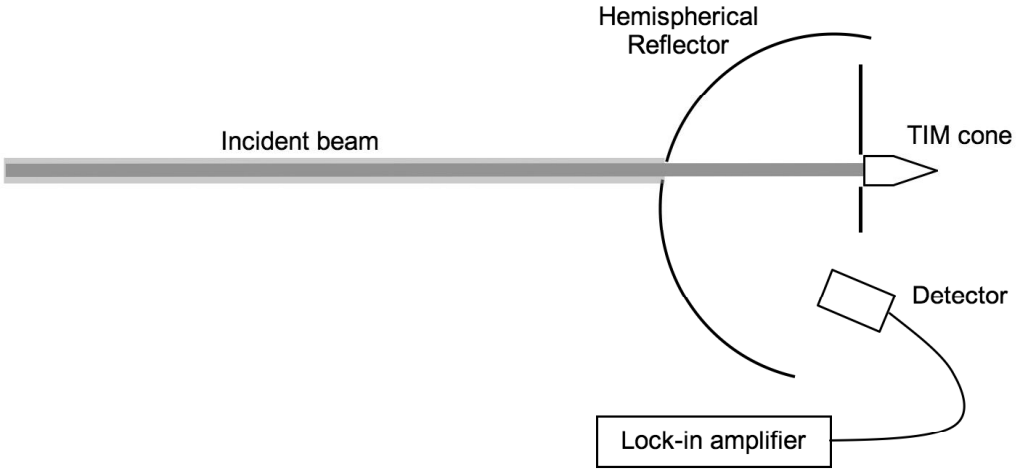

Fig. 5. The layout of the spatially integrated reflectance measurement.

Fig. 5 shows the experimental setup of the spatially integrated reflectance measurement. A 10.6 μm laser is directed over a long path length towards a limiting aperture mounted on the hemispherical reflector that has a size similar to the precision aperture in the TIM instrument. After the limiting aperture an approximately uniform beam is incident onto either a reflectance standard for calibration, or one of the TIM cones for measurement. A 6 mm diameter thin film thermopile detector from Dexter Research is positioned at the opposing focus of the hemisphere to detect the reflectance out of the cone. To facilitate detection, the laser was modulated at 0.5 Hz and the signal from the detector was fed into a lock-in amplifier.

In order to calibrate the reflectance for this measurement, the TIM cone cavity was removed and a diffuse gold reflectance standard was placed a known distance (40 mm) from the aperture with an area equal to the cone entrance. This simple geometry permitted a straightforward calculation of the expected reflectance, 3.4%, using an optical ray-tracing program (Zemax). To perform a measurement of the cavity reflectance, the reflectance standard was removed, and a cone was placed directly behind the aperture. To verify this method of calibration, and to check the detector linearity, the distance between the reflectance standard and the aperture was varied between 25 and 50 mm. The functional form of the measured dependence was then compared to the results generated by the ray-tracing program. An estimation of the uncertainty budget for this measurement is seen in Table 1.

Table 1. Uncertainty budget for the spatially integrated reflectance measurement.

Parameter	**Uncertainty**
Spatial uniformity	11.4%
Reflectance standard	4.0%
Geometry	10.6%
Detector linearity	1.0%
Laser stability	0.5%
RSS	**16.1%**

6. Cavity calibration

For the Glory mission 22 flight-type cones were manufactured with four to be selected for the flight instrument. Measurement of the ESR cavities started early in the production process of the Glory cones, and after each step in the build process a measurement was made at 633 nm which allowed tracking of the stability of the cavity reflectance. Knowledge of the reflectance stability as well as the total absorptance value were drivers in the selection of flight cones.

After completion of the assembly process of the 22 flight-type cavities, reflectance of each was calibrated at the selected wavelengths. To determine the effective cavity reflectance when used for solar irradiance monitoring, the reflectances are weighted by the solar spectrum. The measured reflectance values are fitted over wavelength for each cavity. This fit may be constrained at long wavelengths by estimating a reflectance value at 100 microns that maintains a smoothly varying slope such that the fitted long wavelength reflectance never exceeds unity, and at short wavelengths by the shortest-wavelength reflectance measurement. Since the Sun emits relatively little energy at these far-infrared and ultraviolet wavelengths, the uncertainty in the cavity reflectance from this estimate is low. This uncertainty, as well as those from the fitting parameterization, are accounted for in the measurement uncertainty. For the Glory/TIM cavities, a 2nd degree polynomial nicely fits the reflectance calibration data as shown in Fig. 6. The values of the cavity reflectances are given in Table 2 with the uncertainties described in §7.

Table 2: Glory/TIM solar weighted cavity reflectances

Cavity	**Cavity A**	**Cavity B**	**Cavity C**	**Cavity D**
Reflectance [ppm]	223.1	431.6	351.3	228.8
Uncertainty [ppm]	42.3	81.9	66.7	50.7

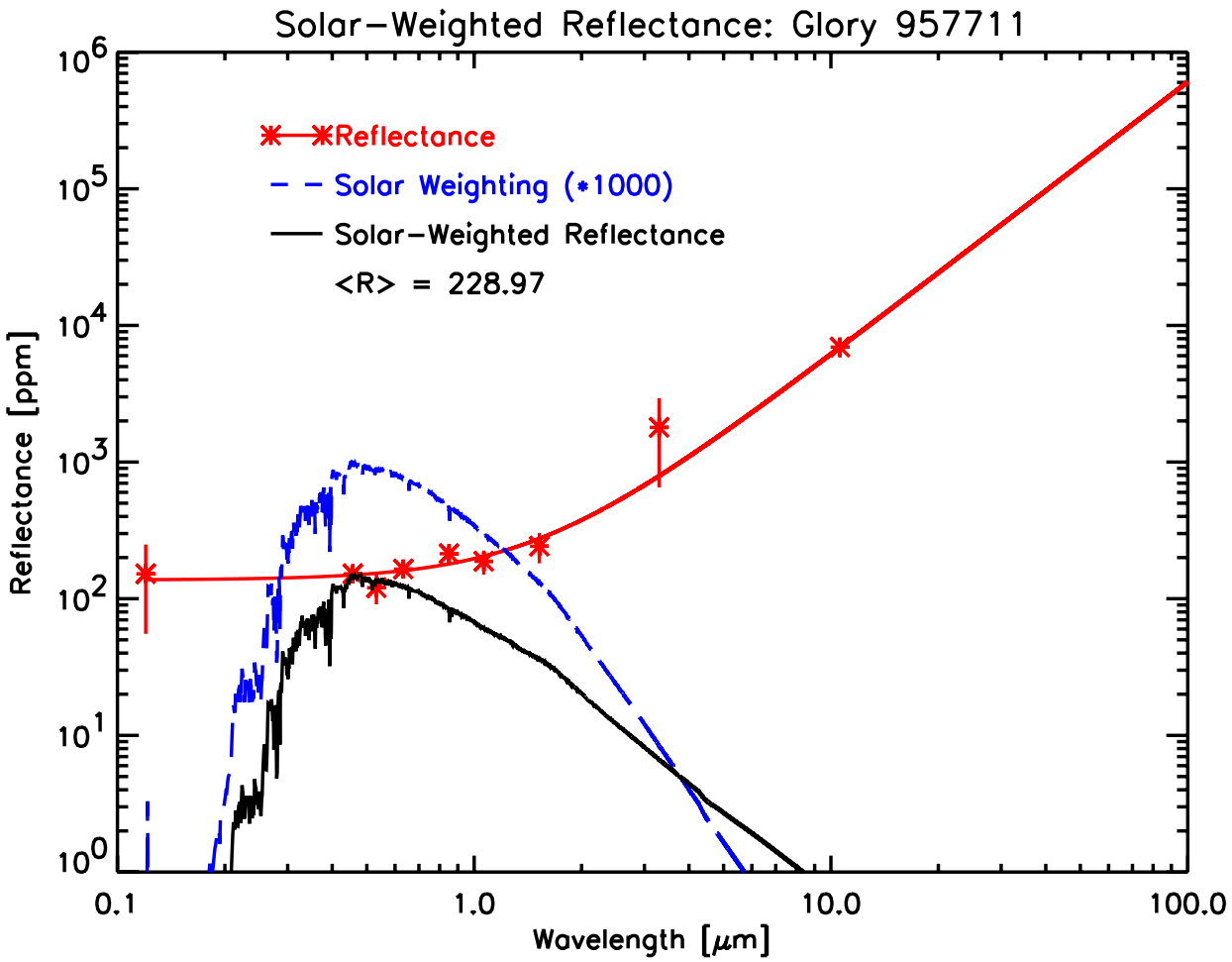

Fig. 6. *The cavity reflectance, smoothly fitted between calibrations at discrete laser (asterisks), increases with wavelength in the infrared. Cavity reflectance is weighted by the normalized solar spectral irradiance (dashed line), giving a relative solar-weighted cavity reflectance (solid line). The integral of this solar weighted reflectance gives the average cavity reflectance used to correct for sunlight not absorbed by the cavity.*

7. Uncertainty budget (spatially mapped)

Several key sources affecting the accuracy of the measurement facility are identified in Table 3. Testing was done to quantify them as they apply to the measurement facility. One parameter would be varied at a time in situ and the deviance from a baseline measurement (where all parameters remained fixed) estimates the effect. Baseline measurements were taken at the beginning of each day of testing and would be used as the comparison standard as well as becoming an element of the "repeatability" distribution. In some cases, numerical methods were used to estimate sensitivities. Most sources are systematic, causing a change that shifts the results. Other sources such as laser stability would add a statistical uncertainty to the result but not bias the results in a certain direction. Most unrecognized sources of uncertainty, such as temperature or humidity, are encompassed in a parameter called "repeatability," which represents the statistical fluctuations of the baseline measurements.

Table 3. Uncertainty sources of the reflectance measurement facility

Uncertainty Source	Error Type	Description	Estimation Procedure
Laser stability	Statistical	Sensitivity to laser intensity change over the measurement time	Compute average laser intensity of multiple detector maps, find σ of these averages.
Laser polarization	Systematic	Bias due to laser polarization orientation	Compare results when using laser polarized in two different orientations
Cone centering	Systematic	Sensitivity to aligning beam in center of cone aperture	Take data with cone deliberately misaligned by 0.5 mm in X and Y, compare to baseline
Orientation of cone - Tip/tilt	Systematic	Sensitivity to aligning cone tip to beam normal	Compare results with different tilt
Orientation of cone - azimuthal	Systematic	Sensitivity to rotational orientation in cone holder	Compare results with different rotation in cone holder
Detector linearity	Systematic	Linearity over dynamic range	Value from literature
Detector position - perpendicular	Systematic	Sensitivity to detector/cone misalignment in X and Y	Numerically shift detector/cone alignment and find σ
Detector position – distance to cone	Systematic	Sensitivity to detector distance from cone	Vary position of detector array to cone and compare results
Detector rotation – azimuthal	Systematic	Sensitivity to detector rotation around beam axis	Numerically rotate detector map in front of cone, compare results
Detector rotation – about vertical	Systematic	Sensitivity of placing detector array parallel to cone aperture	Rotate detector 3° and compare results
Stray light	Systematic	Variation due to background room light	Take data with computer monitor on and off
Baffle position	Systematic	Sensitivity to light baffle position	Compare results with the light baffle in different positions
Chopper speed	Systematic	Sensitivity to frequency of chopped light	Compare runs with the beam chopped at different frequencies
Photodiode noise	Statistical	Sensitivity to noise in photodiode monitor	Compute σ of photodiode signal
Beam splitter	Systematic	Sensitivity to position of laser in beam splitter	Compare results from the laser at different positions in the beam splitter
Beam position in chopper	Systematic	Sensitivity to position of beam in chopper wheel	Compare results from different positions of beam in chopper wheel
Operator	Statistical	Variation due to operator	Compare results from runs taken by different people
Repeatability	Statistical	Stability of redundant runs	Look at statistical distribution for redundant data sets

Table 4 shows the uncertainty budget as function of laser wavelength for the cone reflectance measurements. Most of the parameters are independent of wavelength except for laser stability, beam positioning, and detector linearity. Laser stability was analyzed from the average intensity change of multiple detector maps (where the laser directly illuminated the detector) added in quadrature with short-term fluctuations from the monitor photodiode. For wavelengths where the laser intensity deviated greatly from the detector monitor, the reflectance was computed using the uncorrected laser intensity and a larger uncertainty included to represent this fluctuation in laser stability. The uncertainty for beam positioning for the 1064 nm, 1523 nm, and the 3390 nm wavelengths is greater since the beam was not clearly visible and harder to align particularly for the two longer wavelengths using different detector arrays.

Table 4. The cone reflectance uncertainty budget as a function of wavelength

Parameter \ Wavelength [nm]	457	532	633	850	1064	1523	3390	10600
laser stability	3.75%	20.54%	0.40%	1.20%	6.36%	0.32%	5.49%	Reference table 1.
laser polarization orientation	3.43%	3.43%	3.43%	3.43%	3.43%	3.43%	3.43%	
cone centering	7.74%	7.74%	7.74%	7.74%	15.48%	15.48%	15.48%	
orientation of cone - tip/tilt	5.78%	5.78%	5.78%	5.78%	5.78%	5.78%	5.78%	
orientation of cone - azimuthal	5.44%	5.44%	5.44%	5.44%	5.44%	5.44%	5.44%	
detector linearity	1.00%	1.00%	1.00%	1.00%	1.00%	2.00%	60.00%	
detector position - perpendicular	2.78%	2.78%	2.78%	2.78%	2.78%	11.12%	5.56%	
detector position - distance to cone	3.22%	3.22%	3.22%	3.22%	3.22%	12.88%	6.44%	
detector rotation - azimuthal	0.03%	0.03%	0.03%	0.03%	0.03%	0.03%	0.03%	
detector rotation - vertical	2.05%	2.05%	2.05%	2.05%	2.05%	2.05%	2.05%	
stray light sources	0.88%	0.88%	0.88%	0.88%	0.88%	0.88%	3.52%	
baffle position	0.01%	0.01%	0.01%	0.01%	0.01%	0.01%	0.01%	
chopper speed	0.01%	0.01%	0.01%	0.01%	0.01%	0.01%	0.01%	
photodiode noise	0.00%	0.00%	0.00%	1.19%	2.42%	0.00%	0.00%	
beam splitter	0.41%	0.41%	0.41%	0.41%	0.41%	0.41%	0.41%	
beam position in chopper	0.55%	0.55%	0.55%	0.55%	0.55%	0.55%	0.55%	
operator	0.11%	0.11%	0.11%	0.11%	0.11%	0.11%	0.11%	
repeatability	3.64%	3.64%	3.64%	3.64%	3.64%	3.64%	3.64%	
RSS	**13.66%**	**24.38%**	**13.14%**	**13.24%**	**19.96%**	**25.03%**	**63.62%**	**16.10%**

The uncertainties had a wide dependence on wavelength ranging from 13% in the visible to 63% in the near IR. The 532 nm measurement at 24% was high for the visible and was caused by large fluctuations in the laser intensity. Unfortunately the laser intensity could not be corrected since the laser photodiode monitor did not track the laser accurately for this data set. The 3390 nm measurement had the highest uncertainty at 64% and was dominated by the detector linearity; there is evidence that the detector may have been saturated during the detector sensitivity map.

These uncertainties at individual wavelengths are used in computing the fit to the spectral dependence of each cavity's reflectance, which is then used in computing the solar-weighted reflectance. The fitting introduces additional uncertainties that are estimated at 14% based on sensitivity to fitting parameter and long- or short-wavelength constraints placed on the fit. These contribute to the overall uncertainties given in Table 2.

8. Conclusions

The described calibration facility was used to determine the reflectances of the Glory TIM ESR cavities as a function of seven wavelengths. An uncertainty budget was constructed for this measurement technique giving a level of confidence on the reported values. An additional measurement at 10.6 μm was described along with an estimate of the uncertainty in making this measurement. A functional form was found that fits the reflectance data at each wavelength, which when weighted by the solar spectrum, determines the effective cavity reflectance. Reflectance values for the four Glory/TIM flight cavities are presented with uncertainties for each.

References

1. Kopp, G. and Lawrence G.M., "The Total Irradiance Monitor (TIM): Instrument Design," *Solar Physics* (2005) 230: 91-109
2. Kopp, G., Heuerman K., and Lawrence, G.M., "The Total Irradiance Monitor (TIM): Instrument calibration," *Solar Physics* (2005) 230:111-127
3. Lean, J., *Geophys. Res. Lett*. (2000), 27, 16
4. Hanssen, L.M., Khromchenko, V., Prokhorov, A. and Mekhontsev, S., in *Proceedings of the 2003 CALCON Program*, (2003), Logan, UT.